

# Experimental Demonstration of Underwater Optical Ranging with Enhanced Accuracy Under Scattering Conditions Using Multiple Bessel Modes

Zile Jiang<sup>1\*</sup>, Muralekrishnan Ramakrishnan<sup>1</sup>, Huibin Zhou<sup>1</sup>, Xinzhou Su<sup>1</sup>, Yuxiang Duan<sup>1</sup>, Hao Song<sup>1</sup>, Ruoyu Zeng<sup>1</sup>, Yingning Wang<sup>1</sup>, Robert Bock<sup>2</sup>, Moshe Tur<sup>3</sup>, and Alan E. Willner<sup>1,4</sup>

1. Dept. of Electrical Engineering, University of Southern California, Los Angeles, CA 90089, USA, \*zilejian@usc.edu

2. R-DEX Systems, Inc., Woodstock, GA, 30188, USA

3. School of Electrical Engineering, Tel Aviv University, Ramat Aviv 69978, ISRAEL

4. Dornsife Dept. of Physics & Astronomy, University of Southern California, Los Angeles, CA 90089, USA

**Abstract:** We demonstrate a structured beam-based underwater optical ranging system through scattering, and we utilize multiple ( $>2$ ) Bessel modes for accuracy enhancement. The average error decreases from  $\sim 16$  mm to  $\sim 3$  mm when the number of modes increases from 2 to 8.

## 1. Introduction

A key application of optics is determining distances to an object, i.e., ranging. Indeed, LIDAR-based approaches abound in terrestrial applications through the air [1–3]. Typically, a narrow optical pulse is transmitted, and the reflection is detected. The distance can then be calculated fairly accurately using time-of-flight measurements [4]. This scenario changes for underwater environments. Specifically, a turbid underwater medium will introduce not only significant loss but also a temporal spreading of the transmitted pulses, which introduces a degradation in the distance accuracy of the time-of-flight method [5,6].

An approach was recently reported that combined two different modalities to potentially increase the accuracy of underwater optical ranging [7]. These modalities include: (a) the 2-dimensional spatial distribution of the intensity of a structured beam will rotate as it propagates along the  $z$  direction [8–10], and (b) the beam's spatial distribution is relatively stable through propagation under scattering conditions [11,12]. That demonstration transmitted a beam containing two Bessel modes – thereby producing a rotating petal-like structure – through an underwater scattering medium, where the distance is determined by measuring the angular rotation of the petals of the beam.

In this paper, we experimentally demonstrate a 0.4-meter underwater optical ranging system under scattering conditions utilizing multiple ( $>2$ ) Bessel modes instead of two for performance enhancement. While retaining the rotation characteristics, the structured beam consisting of multiple modes will have two advantages over the 2-mode beam for ranging applications: (a) higher peak power and (b) narrower angular width of the petals. We experimentally generate the beams with different numbers of Bessel modes and use them for underwater ranging. Experimental results show the average measurement errors over a 0.4-m distance are 15.9 mm, 5.4 mm, and 3.0 mm using 2-, 4-, and 8-mode beams, respectively, in an aquatic scattering medium with an attenuation coefficient of  $5 \text{ m}^{-1}$ . Simulation results further verify the efficacy of the proposed scheme in a 10-m underwater ranging scenario with an attenuation coefficient of  $0.4 \text{ m}^{-1}$ , in which the average errors are 25.1 cm, 10.3 cm, and 7.7 cm for 2-, 4-, and 8-mode beams, respectively.

## 2. Concept

Figure 1 (a1) shows the structured beam used in the previous work for underwater ranging [7]. The beam consists of two Bessel modes with different orbital angular momentum (OAM) orders  $\ell$  ( $\ell$  is the number of  $2\pi$  phase shifts in the angular direction of the beam [13]) and different longitudinal wavenumbers  $k_z$ . Due to the spatial interference between the two Bessel modes with a difference of 2 in OAM orders, the transverse beam profile features two petal-like patterns. Further, the difference in the longitudinal wavenumbers will induce a relative phase delay between the two modes, resulting in an angular rotation of the petals along the propagation direction  $z$  [8,9]. Figure 1 (a2) shows the proposed approach to combine multiple ( $N > 2$ ) Bessel modes with linearly correlated OAM orders and longitudinal wavenumbers (i.e.,  $\ell_n = 2n - 1$ ,  $k_z^{\ell_n} = k_z^{\ell_1} - (n - 1)\Delta k_z$ ,  $n = 1, \dots, N$ ). Analogous to the Fourier-series case where one can create a narrower time-domain pulse by combining more frequency components, the proposed multi-mode beam has indeed higher peak power and narrower angular extension of the petals than the 2-mode beam. Both features bring benefits to underwater ranging applications. Figure 1 (b) shows the concept of underwater optical ranging based on the proposed  $z$ -dependent rotating beams. The multi-mode beam in Fig. 1 (a2) is generated, propagated, and then reflected back from the object. We use a camera to capture the intensity profile of the reflected beam, based on which the angular rotation can be detected. The reflector distance  $\Delta z$  is obtained via the linear relationship between  $\Delta z$  and the angular rotation  $\Delta\theta$ , given by  $\Delta\theta = \Delta k_z \Delta z / n_{\text{water}}$ , where  $n_{\text{water}}$  is the refractive index of water. We note that this  $\Delta\theta$ - $\Delta z$  relationship is independent of the number of modes. Therefore, for a fixed  $\Delta k_z$ , the dynamic range of the structure beam (i.e., reflector distance to have a 180-degree rotation) will not be affected by combining more modes.

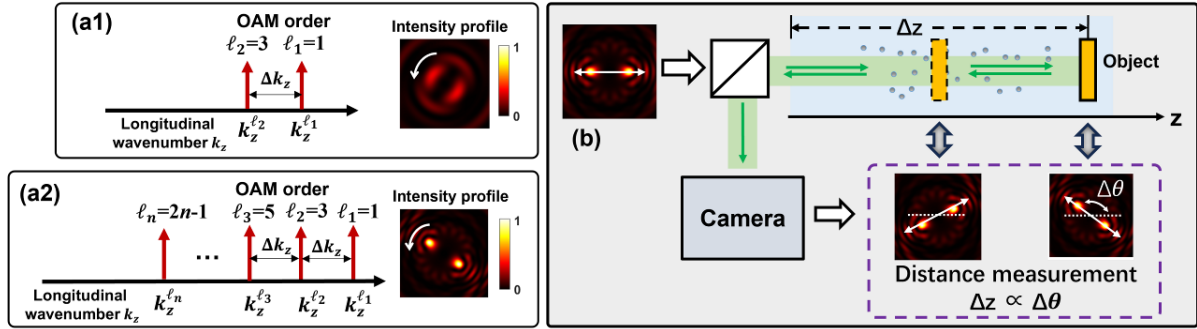


Fig. 1. Structured beams consisting of (a1) two Bessel modes with different longitudinal wavenumber  $k_z$  and OAM order  $\ell$  (the difference in  $\ell$  is 2), and (a2) multiple ( $>2$ ) Bessel modes with linearly correlated  $\ell$  and  $k_z$ . The two intensity profiles in (a1) and (a2) are normalized to have the same total optical power. (b) Concept of using beam with  $z$ -dependent angular rotation for underwater ranging.

Figure 2 (a) shows the simulated and experimentally generated intensity profiles of structured beams consisting of different numbers of Bessel modes. Here  $k_z^1$  and  $\Delta k_z$  are set to be  $1.607 \times 10^7 \text{ m}^{-1}$  and  $4.178 \text{ m}^{-1}$  (resulting in 180-degree rotation for 1-meter reflector distance), respectively for all beams. We use two indicators: (a) peak power and (b) angular petal width to quantify the characteristics of the beams. We convert the beam intensity profile to its angular power distribution by calculating the sum of intensity along each line passing the beam center. The peak power and angular petal width are defined as the maximum and the full width at half maximum (FWHM) of the angular power distribution, respectively. Figures 2 (b1) and (b2) illustrate the experimental and simulation results of the peak power and angular petal width of the beams with different numbers of Bessel modes. We observe that, before the number of modes reaches a specific value (e.g., 8 in our demonstration), the peak power rises while the angular petal width decreases as the number of modes increases. However, after the number of modes exceeds 8, both peak power and petal width do not further improve by adding more modes. Therefore, we may infer that the 8-mode beam should have the highest ranging accuracy in this scenario. An intuitive explanation of this phenomenon is that, due to different OAM orders and radial wavenumbers  $k_r$  (given by  $k_r = \sqrt{(2\pi n_{\text{water}} / \lambda)^2 - k_z^2}$ , where  $\lambda$  is the wavelength), the peak amplitude of each Bessel mode does not efficiently overlap [14]. When the OAM order of the Bessel mode is too high, the peak amplitude deviates too much from other modes and no longer helps improve the peak power of the combined beam.

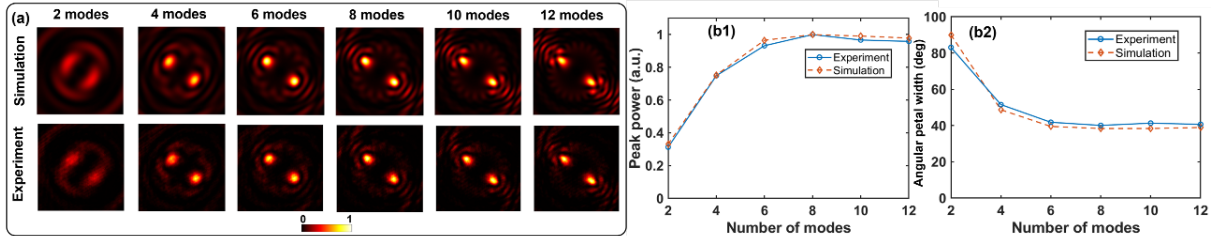


Fig. 2 (a) Experimental and simulated profiles of structured beams consisting of different numbers of Bessel modes. All the profiles are normalized to have the same total optical power. Experimental and simulated (b1) peak power and (b2) angular petal width of beams with different numbers of Bessel modes.

### 3. Experimental Setup and Results

Figure 3 shows the experimental setup of the structured beam-based underwater optical ranging system. We use a spatial light modulator to convert a collimated free-space Gaussian beam into one of the structured beams in Fig. 2 (a). The optical power of the generated beams before entering the water tank is set to be  $\sim -39 \text{ dBm}$  for all beams. The beam then propagates through a tank filled with water and gets reflected back by a mirror. The intensity profile of the reflected beam is captured by a camera for rotation angle detection. The mirror is attached to a linear stage, enabling it to move along the beam propagation direction over a range of 0.4 meters. We add a diluted commercial antacid solution (Maalox®) into the water to emulate the scattering underwater environment. The attenuation coefficient  $\gamma$  is characterized by transmitting a separate Gaussian beam through the scattering medium and measuring the input and output optical power  $P_{\text{in}}$  and  $P_{\text{out}}$ . Based on Beer's law,  $\gamma$  is given by  $\gamma = (\ln P_{\text{in}} - \ln P_{\text{out}}) / L$ ,  $L$  being the path length [15]. We control the scattering strength by varying the concentration of the Maalox® solution. We demonstrate the underwater ranging system under the attenuation coefficients of  $2.1 \text{ m}^{-1}$ ,  $5.0 \text{ m}^{-1}$ , and  $7.9 \text{ m}^{-1}$ , which are all higher than the typical value for seawater ( $< 0.2 \text{ m}^{-1}$  at  $520 \text{ nm}$ ) [16].

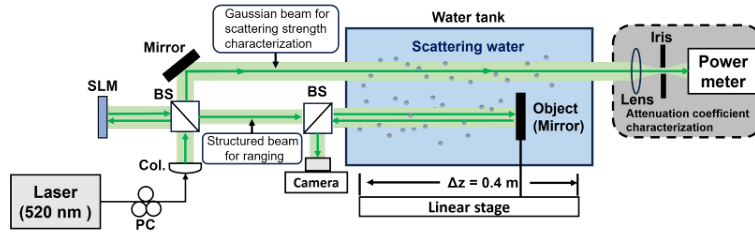


Fig. 3. Experimental setup of the underwater ranging system. Col.: collimator. SLM: spatial light modulator. BS: beam splitter.

Figure 4 (a) shows the measured intensity profiles of the generated 2-mode and 8-mode beams under different attenuation coefficients at distance  $z = 0.4$  m. In the scattering water with  $\gamma = 2.1$  m<sup>-1</sup>, the power loss is  $\sim 7.3$  dB. The beam profiles are not severely distorted compared with those in clear water. Under scattering strength  $\gamma = 5.0$  m<sup>-1</sup>, the two petal-like patterns of the 8-mode beam can still be recognized, while that of the 2-mode beam can hardly be detected. This is because the power of the former is more concentrated than the latter and has higher peak power, making it still detectable under high power loss. Both beams vanish under the strongest scattering where  $\gamma = 7.9$  m<sup>-1</sup> due to  $\sim 27$  dB power loss. Figures 4 (b1) – (b4) illustrate the underwater ranging results using 2-, 4-, and 8-mode beams under different scattering strengths, where the distance measured from the rotation of the beams is plotted versus the actual distance. Under all four cases, the 8-mode beam has higher ranging accuracy than the 2- and 4-mode beams. In clear water and scattering water with  $\gamma = 2.1$  m<sup>-1</sup>, such enhancement mainly benefits from the narrower angular petal width of the 8-mode beam. Fig. 4 (c) shows the average ranging error using 2- to 12-mode beams under different scattering strengths. We observe that in general, the average error first decreases and then increases, where the 8-mode beam gives the minimal error. This trend matches the results of beam peak power and angular petal width in Figs. 2 (b1) and (b2). Specifically, in scattering water with  $\gamma = 5.0$  m<sup>-1</sup>, the average errors are 15.9 mm, 5.4 mm, and 3.0 mm using 2-, 4-, and 8-mode beams, respectively. Finally, in order to verify the effectiveness of the proposed scheme in long distances, we show the simulation results of a 10-meter (beam parameter  $\Delta k_z$  is accordingly modified) ranging system in Figs. 4 (d) and (e), in which the attenuation coefficient is 0.4 m<sup>-1</sup>. Attributed to the higher peak power and narrow petal when combining more modes, the average ranging errors within the 10-m range are 25.1 cm, 10.3 cm, and 7.7 cm when using 2-, 4-, and 8-mode beams, respectively.

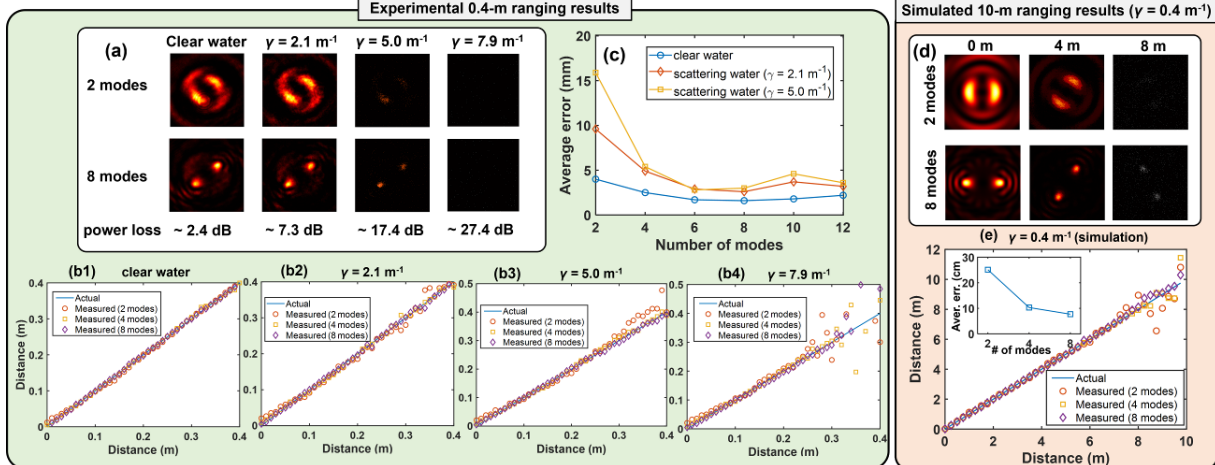


Fig. 4. (a) Measured 2-mode and 8-mode beam intensity profiles at distance  $z = 0.4$  m under different scattering strengths. (b) Experimental 0.4-m ranging results using 2-, 4-, and 8-mode beams in (b1) clear water, and scattering water with (b2)  $\gamma = 2.1$  m<sup>-1</sup>, (b3)  $\gamma = 5.0$  m<sup>-1</sup>, and (b4)  $\gamma = 7.9$  m<sup>-1</sup>. (c) Average ranging error using 2- to 12-mode beams under different scattering strengths. (d) Simulated 2-mode and 8-mode beam intensity profiles at different distances. (e) Simulated 10-m ranging results using 2-, 4-, and 8-mode beams in scattering water with  $\gamma = 0.4$  m<sup>-1</sup>. The inset shows the corresponding average errors.

**Acknowledgment** Office of Naval Research (N6833522C0344); Airbus Institute for Engineering Research.

## References

- [1] C. Rablau et al., Proc. ETOP, 11143-138 (2019);
- [2] M. Jaboyedoff et al., Nat. Hazards, 61, 5 (2012);
- [3] L. Wang et al., J. Lightwave Technol., (2023);
- [4] P. Padmanabhan et al., Sensors, 19, 5464 (2019);
- [5] J. Snow et al., Proc. SPIE Ocean Opt. XI 1750, 418 (1992);
- [6] B. Cochenour et al., IEEE J. Ocean. Eng. 38, 730 (2013);
- [7] H. Song et al., Proc. OFC, M3F.4 (2023);
- [8] A. H. Dorrah et al., Light Sci. Appl. 7, 1 (2018);
- [9] A. Dudley et al., JOSA A, 29, 567 (2012);
- [10] N. Barbieri et al., JOSA A 28, 1462 (2011);
- [11] X. Chu, Eur. Phys. J. D, 66, 259 (2012);
- [12] K. Morgan et al., J. Opt., 18, 104004 (2016);
- [13] A. Yao et al., Adv. Opt. Photon. 3, 161 (2011);
- [14] F. Bowman, Courier Corporation (2012);
- [15] B. Cochenour et al., Opt. Lett., 35, 2088 (2010);
- [16] B. Nababan et al., Earth Environ. Sci., 944, 012047 (2021).